PROCEEDINGS OF SCIENCE

Search for supersymmetry in final states with photons and missing transverse momentum in pp collisions at 13 TeV using the CMS detector

Peter Major*
for the CMS Collaboration,
Eötvös Loránd University, Budapest
MTA-ELTE Lendület Particle and Nuclear Physics Group
E-mail: pmajor@cern.ch †

Supersymmetry (SUSY) is a theoretically favoured extension of the standard model (SM) since it provides solutions to several open questions. Many models employing gauge mediation (GMSB or GGM) predict the production of events with photons and significant missing transverse momentum. In this paper the results of three new searches for SUSY and a combination analysis are reported. The data sample corresponds to an integrated luminosity of 35.9 fb^{-1} collected at a centre-of-mass energy of 13 TeV using the CMS detector at the CERN LHC. The results are used to set cross section limits on gluino, squark and gaugino pair production in either the GMSB or the GGM model framework. The GGM model is favoured for the combination of the search results. By compiling previous results into a single limit setting analysis it is possible to obtain a better sensitivity with respect to individual searches.

XXVII International Workshop on Deep-Inelastic Scattering and Related Subjects - DIS2019
8-12 April, 2019
Torino, Italy

*Speaker.

†The author wishes to thank for their support the Hungarian Academy of Sciences "Lendület" (Momentum) Program (LP 2015-7/2015) and the National Research, Development and Innovation Office of Hungary (K 124845 and K 128713).

PoS(DIS2019)098

1. Introduction

SUSY models depend on a large number of parameters thus in this paper simplified model scenarios (SMS) assuming R-parity conservation are employed to interpret the results. As a consequence non-SM particles are created in pairs and undergo a cascade decay to the lightest supersymmetric particle (LSP) which is stable and assumed to be weakly interacting hence leading to a transverse momentum imbalance (p_T^{miss}) in the detector. The models under consideration use gauge mediated SUSY breaking (GMSB) or general gauge mediation (GGM) to break mass degeneracy of SM particles and their superpartners. In these models, the LSP is the gravitino ($\widetilde{G}$) with a negligible but non-zero mass, while the next-to-LSP (NLSP) is the neutralino ($\widetilde{\chi}_1^0$). In the absence of SUSY phenomena exclusions are derived for the SMS, which can be applied to more complex models that exhibit the same topology. The data sample used corresponds to an integrated luminosity of 35.9 fb^{-1} collected at $\sqrt{s} = 13$ TeV using the CMS [1] detector at LHC.

This paper considers one combined and three individual searches. In Sections 2 and 3 two of the four individual searches are discussed that contribute to the combination paper. The other two [2, 3] were presented at DIS2018 [4]. In Section 4 the combination paper is discussed, finally in Section 5 the latest published individual search is introduced.

2. Strong SUSY Production Leading to Photons and $p_{\text{T}}^{\text{miss}}$ in the Final State

This search [5] considers strong production of either a squark or a gluino pair in the GMSB framework. In both cases the NLSPs are assumed to decay via $\widetilde{\chi}_1^0 \to \gamma + \widetilde{G}$ giving rise to two energetic photons and large $p_{\text{T}}^{\text{miss}}$ in the final state. These processes are described by the T6gg and T5gg simplified model scenarios.

For online event selection the $p_T^\gamma > 30$ (18) GeV, $m_{\gamma\gamma} > 95$ GeV diphoton trigger is used, then offline the presence of two isolated photons with $p_T^\gamma > 40$ GeV, $m_{\gamma\gamma} > 105$ GeV is required at $|\eta| < 1.44$. For selected events $p_{\text{T}}^{\text{miss}} > 100$ GeV and a muon and electron veto are used with $p_T^{e,\mu} > 25$ GeV in the $|\eta| < 2.5$ region. The signal region is then subdivided into six search bins according to $p_{\text{T}}^{\text{miss}}$. Three different SM background contributions are considered. The QCD background is due to jet momentum mismeasurement contributing to $p_{\text{T}}^{\text{miss}}$ and is estimated using an ABCD method. The control regions were created by changing the photons to "fake" photons by inverting some cuts in the photon definition or by requiring $p_{\text{T}}^{\text{miss}} < 100$ GeV. The second background is due to $W \to e\nu$ processes in which the neutrino provides $p_{\text{T}}^{\text{miss}}$ and the electron is misidentified as a γ. It is estimated via the $e \to \gamma$ misidentification rate, measured using the standard Z decay tag and probe method. The third background is due to $Z\gamma\gamma \to \nu\bar{\nu}\gamma\gamma$ and is estimated using simulation.

A non-significant excess of 2.4σ was found in the last $p_{\text{T}}^{\text{miss}}$ bin, hence the exclusion limits are weaker than expected. Figure 1 shows the resulting lower limits, which still provide a 200 GeV improvement over previous analyses, at 1.86 and 1.59 TeV for gluinos and squarks respectively.

3. SUSY Particle Production Leading to a Photon + Lepton + $p_{\text{T}}^{\text{miss}}$ Final State

This analysis [6] considers both strong (T5Wg, T6Wg) and weak (TChiWg) sparticle production. The results are interpreted in the GGM framework. The analysis assumes a mass degeneracy

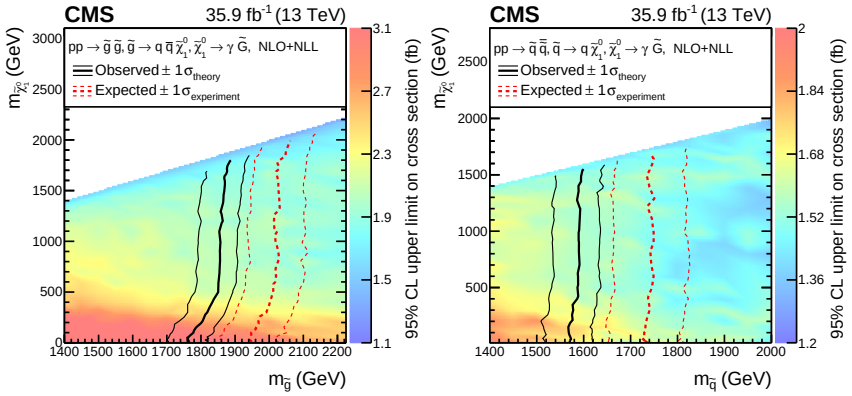

Figure 1: The 95% confidence level expected and observed upper limits on the gluino (left) and squark (right) pair production cross sections as a function of gluino or squark and neutralino masses.

of $\widetilde{\chi}_1^0$ and $\widetilde{\chi}_1^\pm$ and a 50-50% branching fraction in the $\widetilde{g} \to qq\widetilde{\chi}_1^0/\widetilde{\chi}_1^\mp$ and $\widetilde{q} \to q\widetilde{\chi}_1^0/\widetilde{\chi}_1^\mp$ processes and a 100% branching fraction of $\widetilde{\chi}_1^0 \to \gamma\widetilde{G}$ and $\widetilde{\chi}_1^\pm \to W^\pm\widetilde{G}$.

The search is performed in both the $e\gamma$ and $\mu\gamma$ channels. Events are required to have $p_{\mathrm{T}}^{\mathrm{miss}} > 120$ GeV and for the transverse invariant mass of the lepton and the $p_{\mathrm{T}}^{\mathrm{miss}}$ we have $M_T > 100$ GeV. Moreover a photon with $p_T^\gamma > 35$ GeV is required in the $|\eta| < 1.44$ region farther than $\Delta R = 0.3$ from any reconstructed electron or muon and the highest p_T photon has to be farther than $\Delta R = 0.8$ from the highest p_T lepton. The $e\gamma$ sample is selected using the $p_T^\gamma > 30\,(18)$ GeV, $m_{\gamma\gamma} > 95$ diphoton trigger and requiring an electron with $p_T^e > 25$ GeV and $m_{e\gamma} > 100$ GeV for $|\eta| < 2.5$. The $1.44 < |\eta| < 1.56$ region is not used for electrons. The $\mu\gamma$ sample uses a combination of two $\mu\gamma$ triggers. These are $p_T^\mu > 17\,(38)$ GeV and $p_T^\gamma > 30\,(38)$ GeV with (no) photon isolation criteria. In addition a muon with $p_T^\mu > 25$ GeV is required in the $|\eta| < 2.4$ region.

The SM backgrounds are classified as "backgrounds from misidentified photons" and "EWK and misidentified-lepton backgrounds". The $e \to \gamma$ rate is measured via a $Z \to e^+e^-$ tag and probe method, while the jet $\to \gamma$ misidentification rate is estimated using MC. In the second category the EWK $V + \gamma$ background is estimated together with the misidentified lepton contribution using a two component template fit. The distribution shapes of the two backgrounds comes from MC and a control region respectively.

The $e\gamma$ and $\mu\gamma$ signal regions are further divided into 18-18 search bins in $p_{\mathrm{T}}^{\mathrm{miss}}$, H_T and p_T^γ. As no significant excess is observed, upper limits on the signal cross sections are derived for each SMS. Figure 2 shows that for EWK production the NLSP is excluded up to 930 GeV, while according to Figure 3 the strong production channels exclude gluinos below 1.75 TeV and squarks below 1.43 TeV.

4. Combined Search with Photons

The results [7] make use of the signal regions and background estimations of four individual analyses two of which are discussed in Sections 2 and 3. The other two [2, 3] are discussed in [4]. The disjointness of the analyses is ensured by using additional vetoes in an optimised manner. In total 49 search bins are used for most of which the data and the expected counts are in good

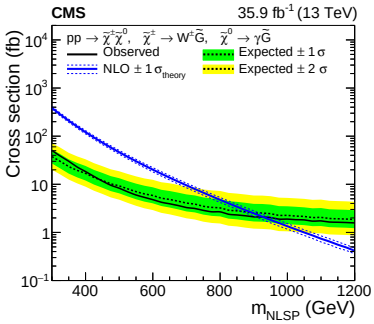

Figure 2: Upper limits on the $\widetilde{\chi}_1^0\widetilde{\chi}_1^{\pm}$ production cross section as a function of the degenerate m_{NLSP}.

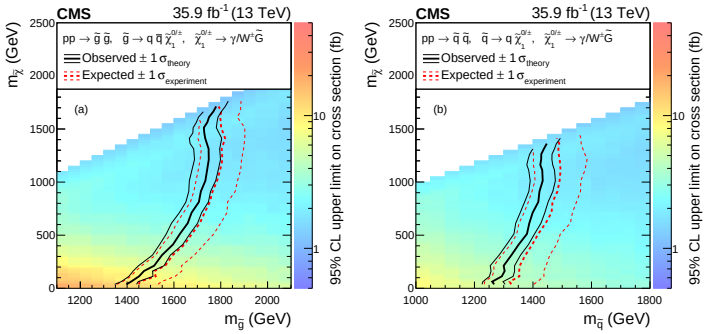

Figure 3: The 95% confidence level upper limits on the gluino (left) and squark (right) pair production cross sections as a function of gluino or squark and neutralino masses.

agreements. The deviations observed in a few bins are not due to the combination. As no significant excess is found upper limits on the SUSY cross sections are calculated. The results are interpreted in the GGM framework using several models.

Figure 4 shows the expected exclusion on the bino-wino mass plane (M_1 and M_2 respectively) with the name of the most sensitive analysis over each region (left) and the same exclusions on the physical $\widetilde{\chi}_1^0$ - $\widetilde{\chi}_1^{\pm}$ mass plane with observed data (right). For low $\widetilde{\chi}_1^0$ masses an improvement of 30 GeV is achieved but not for higher masses due to a small excesses in the signal region. Figure 5 shows the derived exclusions on the NLSP mass as a function of the $\widetilde{\chi}_1^0 \to \widetilde{G}\gamma/Z$ and the $\widetilde{\chi}_1^{\pm} \to (\widetilde{\chi}_1^0 + \mathrm{soft})/(W^{\pm}\widetilde{G})$ branching fractions. In the latter case $\widetilde{\chi}_1^0 \to \widetilde{G}\gamma$ is assumed. The largest improvement is found at BF($\widetilde{\chi}_1^{\pm} \to \widetilde{\chi}_1^0 + \mathrm{soft}$)=40% where the sensitivity of three out of the four analyses are of the same order.

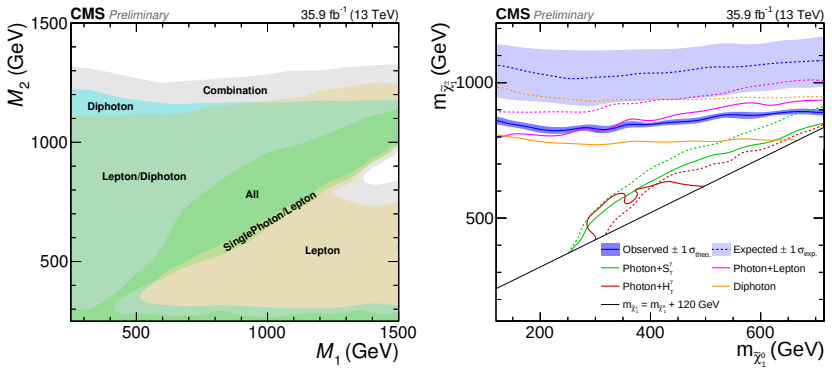

Figure 4: The 95% confidence level upper limits in terms of the GGM model parameters (left) and the physical $\widetilde{\chi}_1^0$ and $\widetilde{\chi}_1^{\pm}$ masses (right). The left panel shows the expected exclusion, while the right panel shows both the observed and the expected exclusion limits.

The results from SMSs with gluino pair production are shown in Figure 6. An exclusion in the $\widetilde{g}$ - $\widetilde{\chi}_1^{0\pm}$ mass plane is obtained by assuming a 50-50% branching fraction in the $\widetilde{g} \to qq\widetilde{\chi}_1^0/\widetilde{\chi}_1^{\pm}$ decay (left). On the right a limit on the NLSP mass is shown as a function of the aforementioned branching fraction at a fixed gluino mass of 1950 GeV.

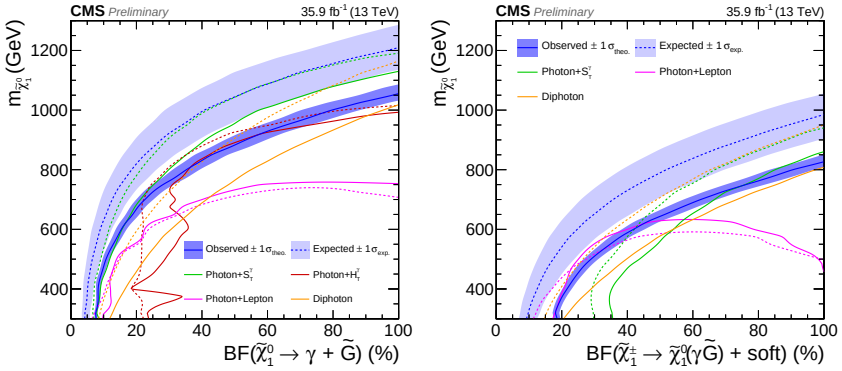

Figure 5: Combined exclusion for the model which probes $\widetilde{\chi}_1^{\pm}\widetilde{\chi}_1^0$ and $\widetilde{\chi}_1^{\pm}\widetilde{\chi}_1^{\pm}$ production combined with the NLSP branching fraction scanned between decays to $Z\widetilde{G}$ and $\gamma\widetilde{G}$ (left). Combined exclusion for the model which probes $\widetilde{\chi}_1^{\pm}\widetilde{\chi}_1^{\pm}$ production combined with the chargino branching fraction scanned between decays to $W\widetilde{G}$ and $\widetilde{\chi}_1^0$+soft. In both cases it is assumed that only the mentioned two decay channels are possible.

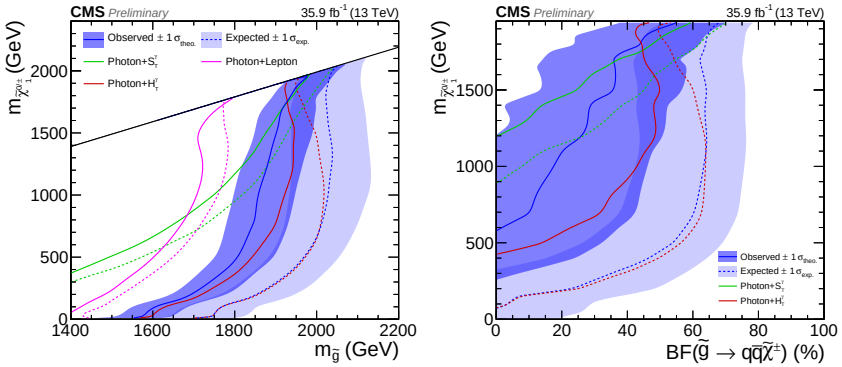

Figure 6: Combined exclusion for the gluino pair production scenario (left) assuming 50-50% probabilities for the $\widetilde{\chi}_1^{\pm}$ and $\widetilde{\chi}_1^0$ production in gluino decay. For the right plot the ratio of the probabilities for both decays are scanned (assuming only these two decays are possible) and the gluino mass is fixed to 1950 GeV.

5. Strong SUSY Production with a Photon, B-jets and p_T^{miss} in the Final State

In this analysis [8] four SMSs of gluino and stop production are considered, all in the GMSB framework. In the $\widetilde{g}\widetilde{g}$ production scenario the gluinos can decay as $\widetilde{g} \to \widetilde{\chi}_1^0 + qq/bb/tt$ which are described by the models T5qqqqHG, T5bbbbZG, T5ttttHG, where $\widetilde{\chi}_1^0 \to \widetilde{G} + (H/\gamma)/(Z/\gamma)/(H/\gamma)$ respectively. The stop pair production scenario is described by the T6ggZG model.

Events are selected using a photon trigger requiring $p_T^{\gamma} > 90$ GeV if $H_T = \sum p_T^{jet} > 600$ GeV and $p_T^{\gamma} > 165$ GeV otherwise. Based on the trigger criteria photons are required to have $p_T^{\gamma} > 100$ GeV if $H_T = \sum p_T^{jet} > 800$ GeV or $p_T^{\gamma} > 190$ GeV if $H_T = \sum p_T^{jet} > 500$ GeV. The event has to have $p_T^{\text{miss}} > 100$ GeV, two jets and no light leptons with $p_T > 10$ GeV nor any isolated electron, muon or charged hadron tracks with $p_T > 5, 5, 10$ GeV. The most energetic jets and the p_T^{miss} are required to have an angular separation of $\Delta\phi > 0.3$. The signal region is divided into 25 search bins based on p_T^{miss}, H_T and the number of b-tagged jets.

The analysis considers four SM backgrounds. The dominant background is due to undetected leptons or hadronic τ decays. These are calculated by extrapolating from a control region where

a light lepton is required using MC. The second background arises from $W \to e\gamma$ events where the electron is misidentified as a photon. This is estimated by extrapolating from a single-electron (zero-photon) control region using the misidentification rate derived from a combination of simulation and data. The third background, due to $Z(\nu\overline{\nu})\gamma$, is calculated from $Z(l^+l^-)\gamma$ events. The fourth background is due to $\gamma+$jets events and is estimated with the help of MC and data.

The derived exclusions, shown in Figure 7, are in good agreement with the expectations for all of the models probed. For moderate $m_{\widetilde{\chi}_1^0}$, gluino masses are excluded up to 2090, 2120, and 1970 GeV for the $\widetilde{g}\widetilde{g}$ production models respectively, while for $\widetilde{t}\widetilde{t}$ production stop masses as large as 1230 GeV are excluded.

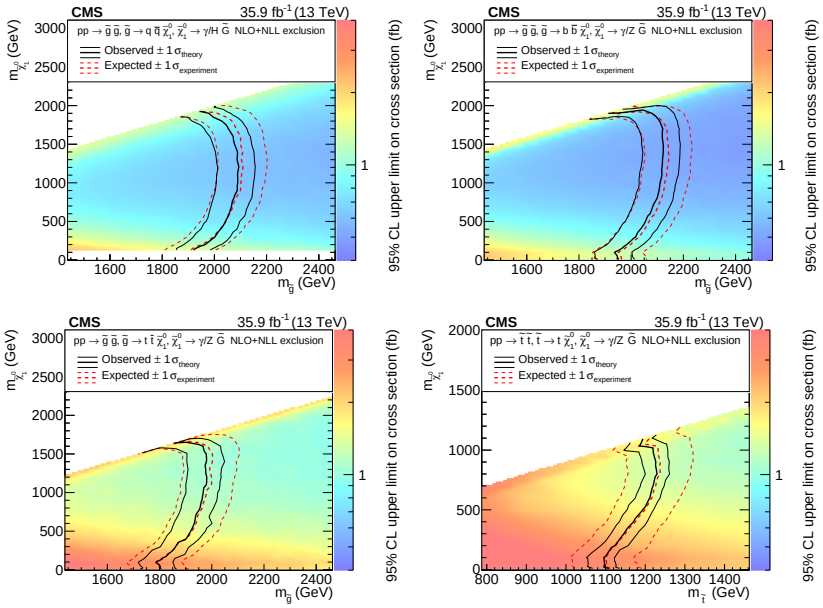

Figure 7: Observed and expected 95% CL upper limits for gluino or top squark pair production cross sections for the T5qqqqHG (upper left), T5bbbbZG (upper right), T5ttttZG (bottom left), and T6ttZG (bottom right) models.

References

[1] CMS Collaboration, JINST 3 (2008) S08004 [DOI:10.1088/1748-0221/3/08/S08004]

[2] CMS Collaboration, Phys. Lett. B 780 (2018) 045 [doi:10.1016/j.physletb.2018.02.045]

[3] CMS Collaboration, JHEP 12 (2017) 142 [doi:10.1007/JHEP12.2017.142]

[4] M. Bartok, PoS DIS2018 (2018) 071, [doi: 10.22323/1.316.0071]

[5] CMS Collaboration, Submitted to: JHEP, arXiv: 1903.07070 [hep-ex].

[6] CMS Collaboration, JHEP **1901** (2019) 154, [doi:10.1007/JHEP01(2019)154]

[7] CMS Collaboration, CMS-PAS-SUS-18-005.

[8] CMS Collaboration, Eur. Phys. J. C **79** (2019) no.5, 444, [doi:10.1140/epjc/s10052-019-6926-x]